Response of Double-Wall Composite Shells to Random Point Loads

D. A. Bofilios*
Rohr Industries, Chula Vista, California
and
R. Vaicaitis†
Columbia University, New York, New York

This paper presents an analytical study of double-wall-laminated fiber-reinforced cylindrical shell response to random loads. A soft viscoelastic core with dilatational modes included is used. The theory of laminated shells is simplified by assumptions similar to those in the Donnell-Mushtari development for isotropic shells. Modal solutions of simply supported shells are obtained. Modal frequencies and deflection response spectral densities are determined. It is found that this approach allows for easy parametric evaluation and that by proper selection of dynamic parameters, viscoelastic core characteristics, and fiber reinforcement orientation, vibration response can be reduced.

Nomenclature

A_{ij}, B_{ij}, D_{ij}	= stiffness coefficients, N/m
$A^{E,I}_{mm}$	= generalized deflection coordinates, m
c_E, c_I	= damping coefficients, N/ms
$C^{(k)}_{ij}$	= elastic moduli, N/m^2
E_a, E_f, E_g, E_p	= elastic moduli of aluminum, fiberglass, graphite, and matrix material, respectively, N/m^2
F^e_j, F^i_j	= point loads acting on external and internal shells, $j=1,2$, N
g_s	= core loss factor
h_k	= distance from reference surface to lamina surface, m
h_s	= core thickness, m
h_E, h_I	= thickness of external and internal shells, m
$H^{E,I}_{mn}$	= frequency response functions of external and internal shells
i,j,k,n,r,s	= indices
i	$=\sqrt{-1}$
k_0	= core stiffness, N/m^3
k_s	$=k_0(1+ig_s)$
L	= length of shell, m
m_s	= mass density of the core, kg/m^3
M	= number of laminae of internal shell
$M_x, M_\theta, M_{x\theta}$	= loading moments, N – m/m
N	= number of laminae of external shell
$N_x, N_\theta, N_{x\theta}$	= membrane forces, N/m
p^e, p^i	= external and internal random pressures, N/m^2
$\bar{p}^{E,I}_{mn}$	= generalized random forces, N/m
q_x, q_w, q_θ	= shell loading, N/m^2
R	= radius of internal shell, m
$RL^{E,I}$	= deflection response levels, dB
$S^e_{F_j}$	= spectral densities of point loads F^e_j, $j=1,2$, N^2/Hz
$S^{E,I}_{mnrs}$	= cross-spectral densities of generalized random forces $\bar{p}^{E,I}_{mn}$, N^2/Hz
u,v,w	= respective displacement in x,θ,r directions, m
w_E, w_I	= displacements of external and internal shells, m
x,θ	= cylindrical coordinates, m, rad
$x^e_j, x^i_j, \theta^e_j, \theta^i_j$	= locations where the point loads are applied, $j=1,2$, m, rad
α	= angle between fiber direction and shell axis, rad
$\zeta^E_{mn}, \zeta^I_{mn}$	= damping coefficients of external and internal shells
ζ_0	= a constant value of damping coefficient
$\mu_a, \mu_f, \mu_g, \mu_p$	= Poisson's ratio of aluminum, fiberglass, graphite, and matrix material, respectively
ρ	= average mass density, kg/m^3
$\rho_a, \rho_f, \rho_g, \rho_p$	= mass densities of aluminum, fiberglass, graphite, and matrix material, respectively, kg/m^3
ρ_E, ρ_I	= mass densities of external and internal shells, kg/m^3
ω	= frequency, rad/s
ω^c_{mn}	= coupled modal frequency of double-wall shell system, rad/s
$\omega^{E,I}_{mn}$	= uncoupled modal frequencies of external and internal shells, rad/s

Superscripts and Subscripts

E,e	= external shell
I,i	= internal shell
E,I	= external or internal shell

Received May 22, 1986; revision received Oct. 31, 1986.

*Research Engineer. Member AIAA.

†Professor, Department of Civil Engineering and Engineering Mechanics. Member AIAA.

Introduction

THE design of many ground and space structures is impacted by the interaction of functional requirements, such as strength, stiffness, weight, passenger and crew comfort, cargo containment protection, reliability, etc. To accommodate many of these requirements, new design concepts for lower weight, extended service life, and reduced cost are needed. It has been demonstrated that composite materials could give weight and structural integrity advantages over many commonly used materials.[1-4] However, the low-weight composites might not provide any advantages with respect to less response, reduced noise transmission,[5] or longer fatigue life. Past studies have demonstrated that sandwich constructions might be an efficient way of dissipating vibrational energy.[6-11] Thus, to satisfy the required vibroacoustic environment, designs utilizing composite materials might need to be modified by including the double-wall sandwich concepts.

This paper presents an analytical study on the vibration response of double-wall circular cylindrical shells of finite extent. Each shell is a composite buildup of laminae, which consists of fibers imbedded in a supporting matrix. Furthermore, each lamina can be oriented in any arbitrary direction. The inputs to the shell are random point loads. The equations of motion are derived using assumptions similar to those given in Refs. 12-17. The viscoelastic core separating the two composite shells is taken to be relatively soft, so that bending and shearing stresses can be neglected, and consequently the core is described by a uniaxial constitutive law. Such a core model allows in-phase (flexural) and out-of-phase (dilatational) motions of the double-wall system.[10,11] The natural frequencies and vibration response are obtained for simply supported cases by modal solutions and a Galerkin-like procedure.

This paper contains numerical results for a simply supported double-wall cylindrical shell. Natural frequencies and vibration response spectral densities are calculated. These results are obtained for double-wall isotropic (aluminum) and double-wall laminated composite cases. The outer shell is constructred from three laminae and the inner shell from ten laminae. It is shown that by proper selection of dynamic parameters, damping characteristics, and reinforcing fiber orientation, lower response values can be obtained for a composite shell than for an equivalent aluminum shell.

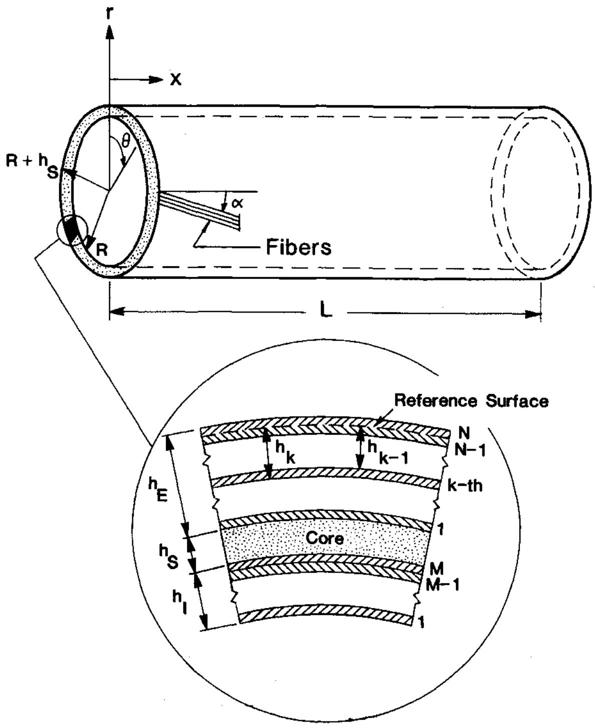

Fig. 1 Geometry of double-wall composite shell.

Response of a Sandwich Shell

The sandwich shell system is composed of two simply supported cylindrical shells and a soft viscoelastic core as shown in Fig. 1. Each shell is constructed from fiber-reinforced laminae of uniform thickness. The fibers are basically the load carriers. A linear viscoelastic model is chosen to describe the behavior of the core. The thin shells separated by the core are modeled according to the theory presented in Refs. 12-17. This theory is appropriate for many arbitrarily oriented layers, each reinfored with unidirectional fibers. The fiber orientation is defined in Fig. 1 with respect to the chosen coordinates.

Following the procedures presented in Refs. 12-17, the equations of motion of a single cylindrical shell are

$$\frac{\partial N_x}{\partial x}+\frac{1}{R}\frac{\partial N_{\theta x}}{\partial \theta}+q_x=\rho\ddot{u} \tag{1}$$

$$\frac{1}{R}\frac{\partial N_\theta}{\partial \theta}+\frac{\partial N_{x\theta}}{\partial x}+\frac{1}{R}\left(\frac{1}{R}\frac{\partial M_\theta}{\partial \theta}+\frac{\partial M_{x\theta}}{\partial x}\right)+q_\theta=\rho\ddot{v} \tag{2}$$

$$\frac{\partial^2 M_x}{\partial x^2}+\frac{2}{R}\frac{\partial^2 M_{x\theta}}{\partial x\partial\theta}+\frac{1}{R^2}\frac{\partial^2 M_\theta}{\partial\theta^2}-\frac{N_\theta}{R}+q_w=\rho\ddot{w} \tag{3}$$

where a dot indicates a time derivative and

$$\begin{bmatrix} N_x \\ N_\theta \\ N_{x\theta} \\ M_x \\ M_\theta \\ M_{x\theta} \end{bmatrix} = \left[\begin{array}{c|c} [A_{ij}] & [B_{ij}] \\ \hline [B_{ij}] & [D_{ij}] \end{array}\right] \begin{bmatrix} \dfrac{\partial u}{\partial x} \\ \left(\dfrac{1}{R}\right)\left(\dfrac{\partial v}{\partial \theta}+w\right) \\ \left(\dfrac{1}{R}\right)\dfrac{\partial u}{\partial \theta}+\dfrac{\partial v}{\partial x} \\ -\dfrac{\partial^2 w}{\partial x^2} \\ -\left(\dfrac{1}{R^2}\right)\left(\dfrac{\partial^2 w}{\partial \theta^2}-\dfrac{\partial v}{\partial \theta}\right) \\ -\left(\dfrac{1}{R}\right)\left(\dfrac{2\partial^2 w}{\partial x\partial\theta}-\dfrac{\partial v}{\partial x}\right) \end{bmatrix} \tag{4a}$$

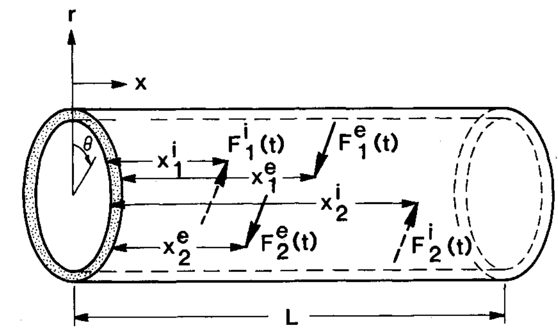

Fig. 2 Random point loads.

where the submatrices $[A_{ij}]$, $[B_{ij}]$, and $[D_{ij}]$ are

$$[(A,B,D)_{ij}]=\begin{bmatrix} (A,B,D)_{11} & (A,B,D)_{12} & (A,B,D)_{16} \\ (A,B,D)_{12} & (A,B,D)_{22} & (A,B,D)_{26} \\ (A,B,D)_{16} & (A,B,D)_{26} & (A,B,D)_{66} \end{bmatrix} \tag{4b}$$

$$\begin{bmatrix} A_{ij} \\ B_{ij} \\ D_{ij} \end{bmatrix} = \sum_{k=1}^{n}[C_{ij}^{(k)}]\begin{bmatrix} (h_k-h_{k-1}) \\ ½(h_k^2-h_{k-1}^2) \\ ⅓(h_k^3-h_{k-1}^3) \end{bmatrix} \tag{5}$$

in which $C_{ij}^{(k)}$ are the elastic moduli of the kth lamina and h_k, h_{k-1} are distances measured from the reference surface to the inner and outer surfaces of the kth lamina (see Fig. 1) and $n=M$ or N. Following Ref. 16, the stiffness coefficients can be calculated in terms of directional moduli, Poisson's ratios, and the fiber orientation angle α. In this approach, the properties of each lamina are functions of volume ratio of fibers to supporting matrix material.

The mass density per unit of surface area is calculated from

$$\rho=\sum_{k=1}^{n}\rho_k(h_k-h_{k-1}) \tag{6}$$

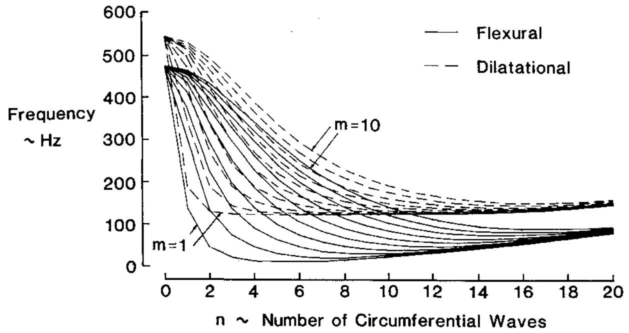

Fig. 3 Modal frequencies of double-wall aluminum shell.

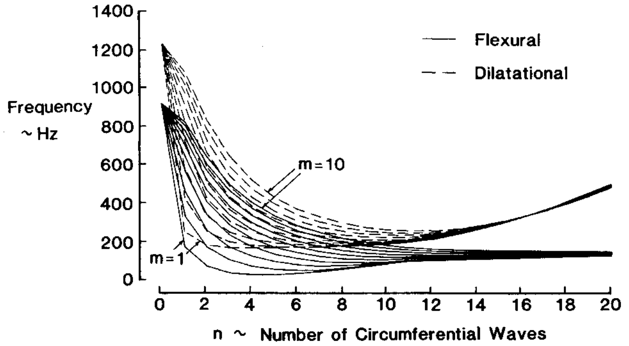

Fig. 4 Modal frequencies of double composite shell.

where ρ_k is the material density of the kth lamina and h_k are distances from reference surface to lamina surface. Setting $q_x = q_\theta = 0$, introducing the Donnell-Mushtari-Vlasov type assumptions,[16,17] and combining Eqs. (1-4a), a single equation in terms of transverse displacement w can be obtained:

$$\{{}_Z\nabla^8 + {}_X\nabla^6 + {}_Y\nabla^4\}w + \nabla^4\{\rho\ddot{w} - q_w\} = 0 \tag{7}$$

$$\begin{aligned}{}_Z\nabla^8 = {} & \frac{Z_1\partial^8}{\partial x^8} + \frac{1}{R}\frac{Z_2\partial^8}{\partial x^7\partial\theta} + \frac{1}{R^2}\frac{Z_3\partial^8}{\partial x^6\partial\theta^2} + \frac{1}{R^3}\frac{Z_4\partial^8}{\partial x^5\partial\theta^3} \\ & + \frac{1}{R^4}\frac{Z_5\partial^8}{\partial x^4\partial\theta^4} + \frac{1}{R^5}\frac{Z_6\partial^8}{\partial x^3\partial\theta^5} + \frac{1}{R^6}\frac{Z_7\partial^8}{\partial x^2\partial\theta^6} \\ & + \frac{1}{R^7}\frac{Z_8\partial^8}{\partial x\partial\theta^7} + \frac{1}{R^8}\frac{Z_4\partial^8}{\partial x^8}\end{aligned} \tag{8}$$

$$\begin{aligned}{}_X\nabla^6 = {} & \frac{1}{R}\frac{X_1\partial^6}{\partial x^6} + \frac{1}{R^2}\frac{X_2\partial^6}{\partial x^5\partial\theta} + \frac{1}{R^3}\frac{X_3\partial^6}{\partial x^4\partial\theta^2} + \frac{1}{R^4}\frac{X_4\partial^6}{\partial x^3\partial\theta^3} \\ & + \frac{1}{R^5}\frac{X_5\partial^6}{\partial x^2\partial\theta^4} + \frac{1}{R^6}\frac{X_6\partial^6}{\partial x\partial\theta^5} + \frac{1}{R^7}\frac{X_7\partial^6}{\partial\theta^6}\end{aligned} \tag{9}$$

$$\begin{aligned}{}_Y\nabla^4 = {} & \frac{1}{R^2}\frac{Y_1\partial^4}{\partial x^4} + \frac{1}{R^3}\frac{Y_2\partial^4}{\partial x^3\partial\theta} + \frac{1}{R^4}\frac{Y_3\partial^4}{\partial x^2\partial y^2} \\ & + \frac{1}{R^5}\frac{Y_4\partial^4}{\partial x\partial\theta^3} + \frac{1}{R^6}\frac{Y_5\partial^4}{\partial\theta^4}\end{aligned} \tag{10}$$

$$\begin{aligned}\nabla^4 = {} & \frac{\alpha_1\partial^4}{\partial x^4} + \frac{2}{R}\frac{\alpha_2\partial^4}{\partial x^3\partial\theta} + \frac{1}{R^2}\frac{\alpha_3\partial^4}{\partial x^2\partial\theta^2} \\ & + \frac{2}{R^3}\frac{\alpha_4\partial^4}{\partial x\partial\theta^3} + \frac{1}{R^4}\frac{\alpha_5\partial^4}{\partial\theta^4}\end{aligned} \tag{11}$$

and the coefficients Z_i, X_j, Y_r, and α_r $(i=1,2,\ldots 9;\ j=1,2,\ldots 7;\ r=1,2,\ldots 5)$ are defined in Ref. 18.

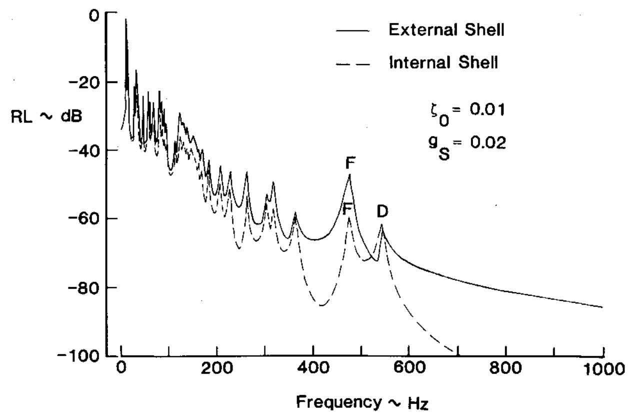

Fig. 5 Deflection response of a double-wall aluminum shell.

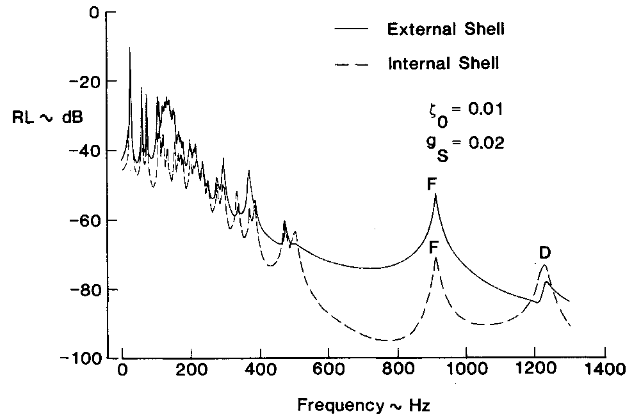

Fig. 6 Deflection response of a double-wall composite shell.

Following Refs. 10 and 11 and using Eq. (7), the double-wall shell motions can be modeled by two coupled partial differential equations for normal deflections w_E and w_I as

$$\begin{aligned}& \{{}_Z\nabla_E^8 + {}_X\nabla_E^6 + {}_Y\nabla_E^4\}w_E + \nabla_E^4\{\rho_E\ddot{w}_E + k_s(w_E - w_I) \\ & + c_E\dot{w}_E + (1/3)m_s\ddot{w}_E + (1/6)m_s\ddot{w}_I\} = \nabla_E^4 p^e(x,\theta,t)\end{aligned} \tag{12}$$

$$\begin{aligned}& \{{}_Z\nabla_I^8 + {}_X\nabla_I^6 + {}_Y\nabla_I^4\}w_I + \nabla_I^4\{\rho_I\ddot{w}_I + k_s(w_I - w_E) \\ & + c_I\dot{w}_I + (1/3)m_s\ddot{w}_I + (1/6)m_s\ddot{w}_E\} = -\nabla_I^4 p^i(x,\theta,t)\end{aligned} \tag{13}$$

The subscripts E, I, and s denote the external and the internal shells and the core, respectively. The p^e and p^i are random loads acting on the external and the internal shell. In the present formulation, the acoustic radiation pressure is not included. The stiffness of the core is represented by a linear viscoelastic spring, $k_s = k_0(1 + ig_s)$, where k_0 is the spring constant and g_s is the loss factor.

The input loads are modeled as random point loads acting at an arbitrary location on the shell surface as shown in Fig. 2. In the vicinity of point load application, some of the assumptions of linear, elastic, thin-shell theory are violated. However, outside the vicinity of the point load, shell response can be calculated with good accuracy. A Dirac delta function is used to define the location of the point load. The random loads p^e and p^i are expressed in terms of two point loads F_1 and F_2 as[17]

$$\begin{aligned}p^e(x,\theta,t) = {} & (1/A_1^e A_2^e)\{F_1^e(t)\delta(x - x_1^e)\delta(\theta - \theta_1^e) \\ & + F_2^e(t)\delta(x - x_2^e)\delta(\theta - \theta_2^e)\}\end{aligned} \tag{14}$$

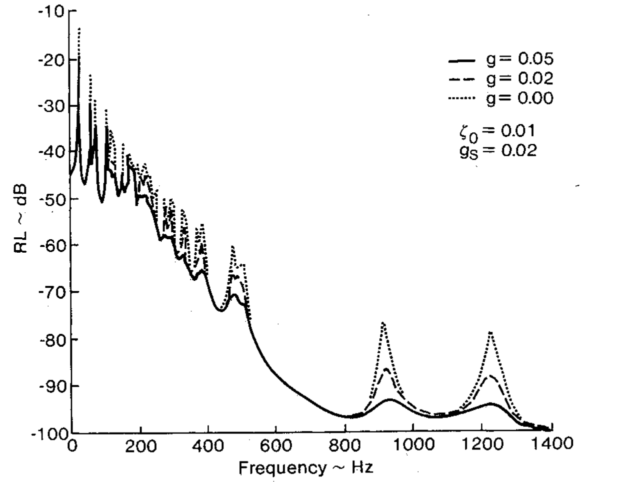

Fig. 7 Response of the exterior shell for several material damping values.

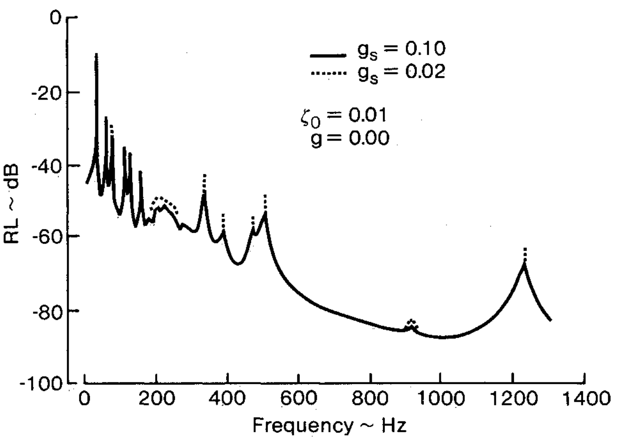

Fig. 8 Response of the interior shell for two values of core damping.

$$p^i(x,\theta,t) = (1/A_1^i A_2^i)\{F_1^i(t)\delta(x-x_1^i)\delta(\theta-\theta_1^i) + F_2^i(t)\delta(x-x_2^i)\delta(\theta-\theta_2^i)\} \tag{15}$$

where the superscripts e and i denote the external and the internal loads, δ is the Dirac delta function, and for a cylindrical shell, $A_1^e=1$, $A_2^e=R+h_s$, $A_1^i=1$, and $A_2^i=R$. The point loads are assumed to be independent, and each is characterized by a spectral density.

The equations of motion of double-wall shells are solved by modal expansion methods. These equations are further simplified by neglecting from the operators ${}_Z\nabla^8$, ${}_X\nabla^6$, ${}_Y\nabla^4$, and ∇^4 the terms containing odd derivatives of spatial variables x and θ. This allows the uncoupling of the modal coordinates, significantly reducing computation time. The general solution of Eqs. (12) and (13) is expressed in terms of the simply supported shell modes

$$w_E(x,\theta,t) = \sum_{m=1}^{\infty}\sum_{n=0}^{\infty} A_{mn}^E X_{mn}^S(x,\theta) \tag{16}$$

$$w_I(x,\theta,t) = \sum_{m=1}^{\infty}\sum_{n=0}^{\infty} A_{mn}^I X_{mn}^S(x,\theta) \tag{17}$$

where A_{mn}^E and A_{mn}^I are the generalized coordinates of external and internal shells and X_{mn}^S are the shell modes. For a simply supported shell, $X_{mn}^S = \sin(m\pi x/L)\cos n\theta$. The input loads p^e and p^i are also expanded in terms of the natural

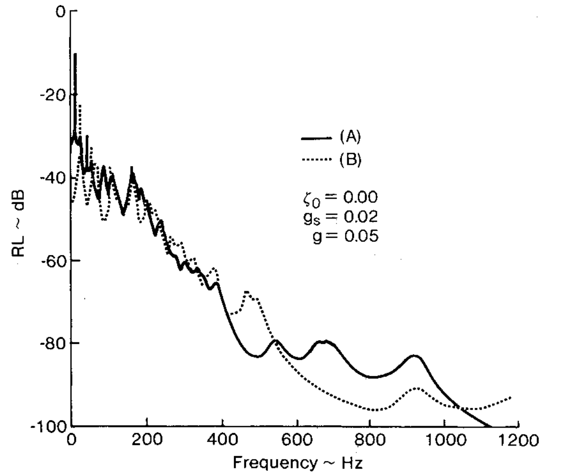

Fig. 9 Response of exterior shell for two different orientations of reinforcing fibers.

shell modes. The substitution of Eqs. (16) and (17) into Eqs. (12) and (13) and the use of the orthogonality principle give a set of coupled differential equations in A_{mn}^E and A_{mn}^I. Taking the Fourier transform of these equations, it can be shown that

$$\bar{A}_{mn}^E = H_{mn}^E\{\bar{P}_{mn}^E/\rho_E + A_{mn}^I(k_s + i\omega c_E + (1/6)m_s\omega^2)/\rho_E\} \tag{18}$$

$$\bar{A}_{mn}^I = H_{mn}^I\{\bar{P}_{mn}^I/\rho_I + \bar{A}_{mn}^E(k_s + i\omega c_I + (1/6)m_s\omega^2)/\rho_I\} \tag{19}$$

in which a bar indicates a transformed quantity. The generalized random forces $\bar{P}_{mn}^E$ and $\bar{P}_{mn}^I$ corresponding to the point loads given in Eqs. (14) and (15) are

$$\bar{P}_{mn}^E = \{\bar{F}_1^e X_{mn}^S(x_1^e,\theta_1^e) + \bar{F}_2^e X_{mn}^S(x_2^e,\theta_2^e)\}/(R+h_s) \tag{20}$$

$$\bar{P}_{mn}^I = \{\bar{F}_1^i X_{mn}^S(x_1^i,\theta_1^i) + \bar{F}_2^i X_{mn}^S(x_2^i,\theta_2^i)\}/R \tag{21}$$

The frequency response functions of the external and internal shells are

$$H_{mn}^E = 1/\{\omega_{mn}^{E2} - \omega^2\gamma_E/\rho_E + i\omega c_E/\rho_E + k_s/\rho_E\} \tag{22}$$

$$H_{mn}^I = 1/\{\omega_{mn}^{I2} - \omega^2\gamma_I/\rho_I + i\omega c_I/\rho_I + k_s/\rho_I\} \tag{23}$$

where

$$\gamma_E = \rho_E + 1/3m_s, \qquad \gamma_I = \rho_I + 1/3m_s$$

$$\begin{aligned}\omega_{mn}^{E,I2} = \{ & Z_1^{E,I}(m\pi/L)^8 + (m\pi/L)^6(Z_3^{E,I}n^2/R_{E,I}^2 - X_1^{E,I}/R_{E,I}) \\ & + (m\pi/L)^4(Z_5^{E,I}n^4/R_{E,I}^4 - X_3^{E,I}n^2/R_{E,I}^3 + Y_1^{E,I}/R_{E,I}^2) \\ & + (m\pi/L)^2(Z_7^{E,I}n^6/R_{E,i}^6 - X_5^{E,I}n^4/R_{E,I}^5 + Y_3^{E,I}n^2/R_{E,I}^4) \\ & + (n/R_{E,I})^4(Z_9^{E,I}n^4/R_{E,I}^4 - X_7^{E,I}n^2/R_{E,I}^3 \\ & + Y_5^{E,I}/R_{E,I}^2)\}/\{\rho_{E,I}[(m\pi/L)^4\alpha_1^{E,I} \\ & + n^2(m\pi/L)^2\alpha_3^{E,I}/R_{E,I}^3 + n^4\alpha_5^{E,I}/R_{E,I}^4]\}\end{aligned} \tag{24}$$

in which the superscripts or subscripts E,I denote either the external or the internal shells, $R_E = R+h_s$, and $R_I = R$, and the parameters $X_i^{E,I}, Y_j^{E,I}, Z_k^{E,I}, \alpha_\ell^{E,I}$ ($i=1,2,...7$; $j=1,2,...5$; $k=1,2,...9$; $\ell=1,2,...5$) are given in Ref. 18.

Equation (24) gives the natural frequencies of uncoupled laminated shell vibrations. The coupled natural frequencies of double-wall shell motions can be obtained from[18]

$$\omega_{mn}^c = \{[-b_{mn} \pm (b_{mn}^2 - 4ac_{mn})^{1/2}]/2a\}^{1/2} \tag{25}$$

where

$$a = \gamma_E \gamma_I - (1/6m_s)^2 \quad (26)$$

$$b_{mn} = (\rho_E \omega_{mn}^{E2} + k_0)\gamma_I + (\rho_I \omega_{mn}^{I2} + k_0)\gamma_E + k_0 m_s/3 \quad (27)$$

$$c_{mn} = (\rho_E \omega_{mn}^{E2} + k_0)(\rho_I \omega_{mn}^{I2} + k_0) - k_0^2 \quad (28)$$

Equation (25) gives two characteristic values for each set of modal indices (m,n). These roots are associated with in-phase flexural and out-of-phase dilatational vibration frequencies of the sandwich construction.

For the analysis presented in this paper, it is assumed that the input spectral densities of the random point loads are specified. Thus, the response (shell deflections) needs to be expressed in the form of a spectral density. Following the procedures given in Ref. 19 and using Eqs. (16) and (17), the spectral densities of normal shell deflection can be obtained from

$$S_w^{E,I}(x,\theta,\omega) = \sum_{m=1}^{\infty}\sum_{n=0}^{\infty}\sum_{r=1}^{\infty}\sum_{s=0}^{\infty} \{\Theta_{mn}^{E,I}(\Theta_{rs}^{E,I})^* S_{mnrs}^{E,I} + \Lambda_{mn}\Lambda_{rs}^* S_{mnrs}^{E,I}\} X_{mn}^s \cdot X_{rs}^s \quad (29)$$

where

$$\Theta_{mn}^{E,I} = (H_{mn}^{E,I}/\rho_{E,I})/\Phi_{mn} \quad (30)$$

$$\Lambda_{mn} = (H_{mn}^E/\rho_E)(H_{mn}^I/\rho_I)(k_s + (1/6)m_s\omega^2)/\Phi_{mn} \quad (31)$$

$$\Phi_{mn} = 1 - (H_{mn}^E/\rho_E)(H_{mn}^I/\rho_I)(k_s + (1/6)m_s\omega^2)^2 \quad (32)$$

$S_{mnrs}^{E,I}$ are the cross-spectral densities of the generalized random forces, and a star indicates conjugate quantity. The cross-spectral densities of the generalized random forces can be determined from Eqs. (20) and (21).

Numerical Results

Numerical results presented herein correspond to the double-wall sandwich shell system shown in Figs. 1 and 2. The following set of parameters are selected for the study: the dimensions of the double-wall shell are $L = 7.62$ m, $R = 1.473$ m, and $h_s = 5.08$ cm. The shell response is computed at $x = L/2$ and $\theta = 45$ deg. The thicknesses of the outer and the inner shell are $h_E = 0.813$ mm and $h_I = 2.54$ mm. The stiffness and material density of the core are $k_0 = 1.14 \times 10^6$ N/m^3 and $\rho_s = 37.40$ Pa-s^2/m^2. The outer shell contains three layers while the inner shell is composed of ten layers. Fiberglass and graphite fibers are used to reinforce the matrix material. The ratio of the fibers volume to the matrix material volume is 0.2. The elastic moduli, Poisson's rations, and material densities are, respectively, $E_f = 5.17 \times 10^{10}$ Pa, $\mu_f = 0.33$, $\rho_f = 2180$ Pa-s^2/m^2, $E_g = 7.03 \times 10^{11}$ Pa, $\mu_g = 0.33$, $\rho_g = 1550$ Pa-s^2/m^2, and $E_p = 1.57 \times 10^{10}$ Pa, $\mu_p = 0.35$, $\rho_p = 1197$ Pa-s^2/m^2. The fiber reinforcement for each layer (the same pattern being used for the inner and outer shell) is arranged as follows: first layer fiberglass, second layer graphite, third layer fiberglass, and so on. For the aluminum shell, $E_a = 7.24 \times 10^{10}$ Pa, $\mu_a = 0.30$, and $\rho_a = 2767.78$ Pa-s^2/m^2.

The damping of the double-wall fiber-reinforced composite shell is assumed to be composed of material damping resulting from internal friction within each of the materials and interfacial slip at the fiber-matrix interfaces, viscous damping caused by radiation effects, and structural damping of the core material. A detailed discussion on the damping of fiber-reinforced composite materials is given in Refs. 20–23. Using the complex elastic modulus approach, we have

$$\bar{E} = E^R(1 + ig) \quad (33)$$

where $\bar{E}$ is the complex modulus, E^R is the real component of $\bar{E}$, and g is the loss factor. The viscous damping coefficients c_E and c_I are expressed in terms of modal damping ratios ζ_{mn}^e and ζ_{mn}^I corresponding to the external and internal shells. As mentioned earlier, damping in the soft core is introduced through the core stiffness $k_s = k_0(1 + ig_s)$ where g_s is the loss factor.

The input random point loads F_j^e, F_j^i $(j = 1,2)$ are assumed to be characterized by truncated Gaussian white noise spectral densities

$$S_{F_1,F_2}^{e,i} = \begin{cases} 4.95 \times 10^{-3}\,\mathrm{N^2/Hz} & 0 < f < 1000\ \mathrm{Hz} \\ 0 & \text{otherwise} \end{cases} \quad (34)$$

Numerical computations were performed using the same value of spectral density for the external and the internal loads. The frequency bandwidth was selected to be $\Delta\omega = 2\pi$ rad/s with the upper cutoff frequency of 6280 rad/s. The random point loads were located at $x_1^e = x_2^e = 3.81$ m, $x_1^i = x_2^i = 3.81$ m, $\theta_1^e = -90$ deg, $\theta_2^e = 90$ deg, $\theta_1^i = -90$ deg, and $\theta_2^i = 90$ deg.

The modal frequencies of double-wall aluminum and double-wall composite shells are presented in Figs. 3 and 4. The fiber reinforcement pattern fiberglass/graphite is repeated for the exterior and interior shells. The fiber orientation for the three layers of the exterior shell are $\alpha = -45$, 45, and -45 deg. The fiber orientation for the ten layers of interior shell is arranged in an alternating order with $\alpha = -45$, 45, -45, and 45 deg.... The results are presented for half-axial wavelengths $m = 1,2,...,10$ and for circumferential waves $n = 0,1,...,20$. The results plotted in Figs. 3 and 4 indicate that for the large shell dimensions and the ratio radius/length = 0.1933 chosen in this study, the modal frequencies at $n = 0$ seem to converge to a single point for all values of $m = 1,2,...,10$.

A comparison of the results obtained from Eq. (24) and from a NASTRAN finite-element program show a reasonable agreement. These results were obtained for a single fiberglass/graphite composite shell composed of ten lamina layers. The lowest modal frequency corresponding to mode number $m = 1$ and $n = 4$ is 32.24 Hz (NASTRAN) and 35.31 Hz [Eq. (24)]. The fiber orientation for the ten layers is $\alpha = -45$, 45, -45, and 45 deg .... A similar level of agreement was obtained for several other lower-order modes. It should be noted that the mode numbers that are assigned to a particular frequency form a NASTRAN output are decided on the basis of the graphic display of the mode shapes.

A comparison of the modal frequencies of aluminum and composite shells indicate that, depending on fiber reinforcement orientation, significantly higher modal frequencies can be obtained for a composite shell. However, the mass of the composite shell is about 50% less than that of the aluminum shell while all the other geometric parameters are the same. For the results that follow, the fiber orientation of the composite shell, except when stated, will be the same as that given for Fig. 4. The deflection response spectral densities of double-wall aluminum and composite shells are given in Figs. 5 and 6. The abscissa is a logarithmic scale, called response level (RL) in units of decibels (dB)

$$RL^{E,I}(x,\theta,\omega) = 10 \log[S_w^{E,I}(x,\theta,\omega)\Delta\omega/w_{\mathrm{ref}}^2] \quad (35)$$

where the reference deflection w_{ref} is taken to be equal to $w_{\mathrm{ref}} = h_E = 0.813$ mn. As can be seen from these results, a large number of flexural and dilatational modes are excited by point loads. Due to a large number of participating modes and modal frequency overlaps as shown in Figs. 5 and 6, it is difficult to identify response peaks corresponding to dilatational frequencies. However, for $n = 0$ the flexural and dilatational frequencies are well separated. A direct comparison of these results indicates that at most frequencies the response levels of the composite shells are lower when compared to the response levels of the aluminum shells.

However, at some frequency values the opposite is true. The results presented in Figs. 5 and 6 were obtained for identical damping conditions of the aluminum and fiber-reinforced composite shells. In this case, the loss factor g for the composite materials was set equal to zero.

To demonstrate the effect of material and core damping, results are presented in Figs. 7 and 8 for a double-wall composite shell but different values of loss factors g and g_s. The viscous damping coefficient $\zeta_0 = 0.01$ and the point loads are acting on the interior shell for both of these cases. By increasing the material loss factor g, significant gains in response reduction can be achieved at most modal frequencies. Only 2–4 dB of response reduction is achieved at some peaks when the damping loss factor of the core g_s is increased from 0.02 to 0.1. However, the shells forming a double-wall construction are bonded to the core. Thus, an increase of viscous properties in the core would increase the modal damping of the face shells. Then the cumulative effect of damping on the vibration response would be much greater than that shown in Fig. 8.

The deflection response levels of the external shell are given in Fig. 9 for two fiber orientations. The loads in this case are acting on the internal shell. The fiber orientation for the two curves are A) $\alpha = - -45$, 45, -45, deg external, $\alpha = -45$, 45, -45, 45 deg, etc (internal), B) $\alpha = 90$, 0, 90, 0 deg, etc. (external), $\alpha = 90$, 0, 90, 0 deg, etc. (internal). For both of these cases it is assumed that material loss factor $g = 0$. A comparison of these results indicates that the response levels are significantly higher at some frequencies when the fiber reinforcement orientation for alternating laminae is orthogonal.

Conclusions

An analytical model has been developed to predict the vibration response of double-wall composite shells to random inputs. The results indicate that shell response is strongly dependent on the damping characteristics of the shell material and the core, location of the point load action, and the reinforcement of the fiber orientation of the different layers. In general, the response levels of a composite shell are lower at most frequencies than those of an equivalent aluminum shell. However, by proper selection of damping and reinforcement of the fiber orientation, additional amounts of response reduction can be achieved by a design composed of two composite shells and a soft viscoelastic core.

Acknowledgment

The work reported here was supported by the NASA Langley Research Center through Grant NAG-1-541.

References

[1]Davis, G. W. and Sakata, I. F., "Design Considerations for Composite Fuselage Structure of Commercial Transport Aircraft," NASA CR-159296, March 1981.

[2]Revell, J. D., Balena, F. J., and Koval, L. R., "Analytical Study of Interior Noise Control by Fuselage Design Techniques on High-Speed, Propeller Driven Aircraft," NASA CR-159222, July 1978.

[3]Yang, J. C. S. and Tsui, C. Y., "Optimum Design of Structures and Composite Materials in Response to Aerodynamic Noise and Noise Transmission," NASA CR-155332, Dec. 1977.

[4]Durchlaub, E. C., "Minimized Fuselage Vibrations Using Advanced Composites," *33rd Annual National Forum of the American Helicopter Society*, Paper 77.33-84, Washington, D.C., May 1977.

[5]Koval, L. R., "Sound Transmission into a Laminated Composite Cylindrical Shell," *Journal of Sound and Vibration*, Vol. 71, Aug. 1980, pp. 523–530.

[6]Freudenthal, A. M. and Bieniek, M. P., "Forced Vibrations of Sandwich Structures," WADD Technical Rept. 60-307, U.S. Air Force, Jan. 1961.

[7]Ford, R. D., Lord, P., and Walker, A. W., "Sound Transmission Through Sandwich Constructions," *Journal of Sound and Vibration*, Vol. 5, Jan. 1967, pp. 9–21.

[8]Smolenski, C. P. and Krokosky, E. M., "Dilatational-Mode Sound Transmission in Sandwich Panels," *Journal of the Acoustical Society of America*, Vol. 54, Dec. 1973, pp. 1449–1457.

[9]Dym, D. L. and Lang, M. S., "Transmission of Sound Through Sandwich Panels," *Journal of the Acoustical Society of America*, Vol. 56, Nov. 1974, pp. 1523–1532.

[10]Vaicaitis, R., "Noise Transmission by Viscoelastic Sandwich Panels, NASA TN D-8516, Aug. 1977.

[11]Vaicaitis, R. and Hong, H.-K., "Nonlinear Response of Double Wall Sandwich Panels," AIAA Paper 83-1037, May 1983.

[12]Bert, C. W., Baker, J. L., and Eagle, D. M., "Free Vibration of Multilayer Anisotropic Cylindrical Shells," *Journal of Composite Materials*, Vol. 3, 1969, pp. 470–499.

[13]Roth, B. K. and Das, Y. C., "Vibration of Layered Shells," *Journal of Sound and Vibration*, Vol. 28, 1973, pp. 737–757.

[14]Harari, A. and Sandman, B. E., "Vibration Response of Laminated Cylindrical Shells Embedded in an Acoustic Fluid," *Journal of the Acoustical Society of America*, Vol. 60, July 1976.

[15]Dong, S. B., "Free Vibration of Laminated Orthotropic Cylindrical Shells, *Journal of the Acoustical Society of America*, Vol. 44, 1968.

[16]Soedel, W., "Simplified Equations and Solutions for the Vibration of Orthotropic Cylindrical Shells," *Journal of Sound and Vibration*, Vol. 87 1983, pp. 555–566.

[17]Soedel, W., *Vibrations of Shells and Plates*, Marcel Dekker, Inc., New York, 1981.

[18]Vaicaitis, R. and Bofilios, D. A., "Response of Double Wall Composite Shells," AIAA Paper 85-0604-CP, April 1985.

[19]Lin, Y. K., *Probabilistic Theory of Structural Dynamics*, McGraw-Hill, New York, 1967, pp. 207–228.

[20]Chang, S. and Bert, C. W., "Analysis of Damping for Filamentary Composite Materials," *Composite Materials in Engineering Design, Proceedings of the 6th St. Louis Symposium*, May 1972.

[21]Bert, C. W., "Composite Materials: A Survey of Damping Capacity of Fiber-Reinforced Composites," *Damping Applications for Vibration Control*, edited by P. J. Jarvik, ASME, AMD, Vol. 38, Nov. 1980.

[22]Bert, C. W., "Material Damping: An Introductory Review of Mathematical Models, Measures and Experimental Techniques," *Journal of Sound and Vibration*, Vol. 29, 1973, pp. 129–153.

[23]Sin, C. C. and Bert, C. W., "Sinusoidal Response of Composite Materials Plates with Material Damping," *Journal of Engineering for Industry, Transactions of ASME*, May 1974, pp. 603–610.